Journal of Photochemistry and Photobiology A: Chemistry 220 (2011) 139–144

Contents lists available at ScienceDirect

Journal of Photochemistry and Photobiology A: Chemistry

journal homepage: www.elsevier.com/locate/jphotochem

Active vibrations of indene cation studied by mass-analyzed threshold ionization spectroscopy

Chaochao Qin[a,c,d], Sheng Yuan Tzeng[a], Bing Zhang[c], Wen Bih Tzeng[a,b,*]

[a] Institute of Atomic and Molecular Sciences, Academia Sinica, P.O. Box 23-166, 1, Section 4, Roosevelt Road, Taipei 10617, Taiwan
[b] Department of Chemistry, National Taiwan Normal University, 88, Sec. 4, Roosevelt Road, Taipei 11677, Taiwan
[c] State Key Laboratory of Magnetic Resonance and Atomic and Molecular Physics, Wuhan Institute of Physics and Mathematics, Chinese Academy of Sciences, Wuhan 430071, China
[d] Graduate School of the Chinese Academy of Sciences, Beijing 100049, China

ARTICLE INFO

Article history:
Received 7 December 2010
Received in revised form 2 March 2011
Accepted 2 April 2011
Available online 12 April 2011

Keywords:
Resonant multi-photon ionization
Threshold ionization
Molecular vibration
Indene
Cation spectrum
Vibronic spectrum

ABSTRACT

We applied the resonant two-photon mass-analyzed threshold ionization (MATI) technique to cation spectra of indene by ionizing via eight different intermediate vibronic levels. The adiabatic ionization energy was determined to be 65 721 ± 5 cm^{-1}. Most of the pronounced MATI bands result from the active vibrations involving in-plane ring deformation motions of the indene cation. Analysis of these MATI spectra suggests that the molecular geometry of the indene cation in the ground D_0 state resembles that of neutral species in the electronically excited S_1 state.

1. Introduction

Zero kinetic energy (ZEKE) photoelectron spectroscopy is one of the major techniques for obtaining information about the properties of molecular ions [1,2]. This method involves the excitation of long-lived high Rydberg states which are ionized in a delayed pulsed electric field, leading to production of threshold ions in well-defined energy states. It gives information about the adiabatic ionization energies (IEs) of molecules as well as the vibrational levels of ions in high precision. However, the ZEKE technique is subject to the detection of electrons and does not contain mass information. In a similar approach, the mass-analyzed threshold ionization (MATI) method involves detection of threshold ions with zero kinetic energy and it provides unambiguous mass-resolved spectral information [3–6].

Indene is a polycyclic hydrocarbon with chemical formular C_9H_8. It is composed of a benzene ring fused with a cyclopentene ring, as seen in Fig. 1. The structure and normal vibrations of indene in the ground S_0 state have been investigated by using the electron diffraction [7], microwave [8], IR [9,10], and far-IR [11] spectroscopic techniques. In addition, the electronic transition has been investigated by vapor phase ultra-violet absorption [12,13] and one-color resonant two-photon ionization (1C-R2PI) spectroscopy [14]. Results from these studies have increased our knowledge about the structures and vibrations of this molecule in the S_0 and electronically excited S_1 states. The IE of indene has been measured by two-color resonant two-photon ionization (2C-R2PI) spectroscopy [14] as well as photoelectron spectroscopy [15,16]. However, the spectroscopic data about the active vibrations and geometry of the indene cation are not yet available in the literature.

In this paper, we report the cation spectra of indene, by using two-color resonant two-photon MATI technique. The experimental data give information about the precise adiabatic IE and the active vibrations in the cationic ground D_0 state. To investigate the existence of possible isomers as well as the molecular geometry and active vibrations of the cation, we have recorded the vibrationally resolved MATI spectra by ionizing through eight intermediate levels in the S_1 state. We have also performed ab initio and density functional theory (DFT) calculations to predict the structures, energies and vibrational frequencies of indene in the S_0, S_1, and D_0 states. The calculated results are found to support the experimental findings.

* Corresponding author at: Institute of Atomic and Molecular Sciences, Academia Sinica, P.O. Box 23-166, 1, Section 4, Roosevelt Road, Taipei 10617, Taiwan. Tel.: +886 2 23668236, fax: +886 2 23620200.
E-mail address: wbt@sinica.edu.tw (W.B. Tzeng).

1010-6030/$ – see front matter © 2011 Elsevier B.V. All rights reserved.
doi:10.1016/j.jphotochem.2011.04.004

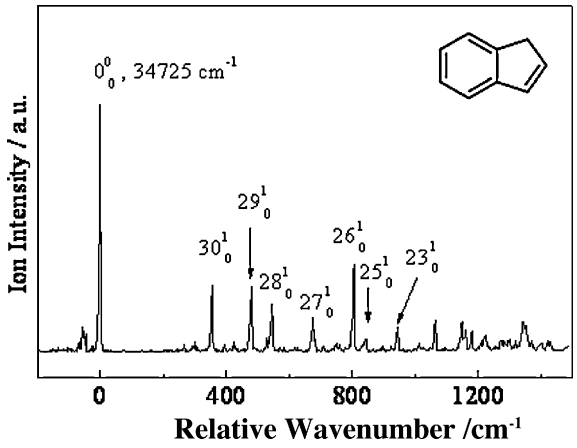

Fig. 1. Vibronic spectrum of indene recorded by the 2C-R2PI method. The spectrum was obtained by scanning the excitation laser while fixing the ionization laser at 31 143 cm^{-1}.

2. Experimental and computational details

2.1. Experimental method

The experiments reported in this paper were performed with a laser-based time-of-flight (TOF) mass spectrometer as described in our previous publication [17]. Indene (99% purity) was purchased from Sigma–Aldrich Corporation and used without further purification. The vapors of the liquid sample kept at room temperature were seeded into 2–3 bar of helium and expanded into the vacuum through a pulsed valve with a 0.15 mm diameter orifice. During the experiments, the gas expansion and the ionization regions were maintained at a pressure of 1×10^{-3} and 1×10^{-5} Pa, respectively.

We initiated the two-color resonant two-photon excitation process by utilizing two independent tunable UV laser systems controlled by a delay/pulse generator (Stanford Research Systems, DG 535). The excitation (pump) source is a Nd/YAG (Quanta-Ray LAB-150) pumped dye laser (Lambda-Physik, Scanmate-2 with BBO-III crystal; R-590 and R-610 dyes) with bandwidth $\leq$0.3 cm^{-1}. The visible radiation is frequency doubled to produce UV radiation. The ionization (probe) UV laser (Lambda-Physik, Scanmate-2 OG with BBO-III crystal; DCM dye) was pumped by a frequency-doubled Nd/YAG (Quanta-Ray LAB-150). A laser wavelength meter (Coherent, WaveMaster) was used to calibrate the wavelengths of both lasers. These two counter-propagating laser beams were focused and intersected perpendicularly with the molecular beam at 50 mm downstream from the nozzle orifice. The intensities of the laser beams were monitored by fast photodiodes and fed a transient digitizer.

In the 2C-R2PI experiments, the total ion signal is collected. Analysis on the rising step in the photoionization efficiency (PIE) curve can yield an IE with an uncertainty of about 10–20 cm^{-1}. In the MATI experiments, both the prompt ions and the Rydberg neutrals were formed simultaneously in the laser and molecular beam interaction zone. A pulsed electric field of −1 V/cm (duration = 10 μs) in this region was switched on about 40 ns after the occurrence of the laser pulses. In such a way, the prompt ions were guided towards the opposite direction of the flight tube and not detected by the particle detector. Because the Rydberg neutrals were not affected by the electric field, they kept moving to the second TOF lens region with a velocity of about 1500 m/s. (See Fig. 1 of Ref. [17] for the schematic diagram of the apparatus.) After a time delay of about 11.2 μs, a second pulsed electric field of +500 V/cm (duration = 10 μs) was applied to field-ionize the Rydberg neutrals. These threshold ions were then accelerated and passed a 1.0 m field-free region before being detected by a dual-stack microchannel plate particle detector. The ion signal from the detector was collected and analyzed by a multichannel scaler (MCS, Stanford Research System, SR430). Each TOF mass spectrum at a particular laser wavelength was accumulated for 300 laser shots and shown on the screen of the MCS. All TOF mass spectra were saved in the PC at a 0.020 nm (equivalent to 1.2 cm^{-1}) spacing over the entire scanning range of laser wavelength. Composite optical spectra of intensity versus wavelength were then constructed from the individual mass spectra. The MCS and the transient digitizer were interfaced to a personal computer. As the detected signal is proportional to the photon intensities of the excitation and ionization lasers for a two-color two-photon process, the obtained optical spectra were normalized to the laser power in order to avoid spurious signals due to shot-to-shot laser fluctuation.

Table 1
Measured and calculated electronic transition and ionization energies (in cm^{-1}) of indene.

	$S_1 \leftarrow S_0$	IE	Deviation (%)
Experimental method			
2C-R2PI	34 725 ± 2		
2C-R2PI		65 715 ± 10	
MATI		65 721 ± 5	
Computational method			
CIS/6-311++G**	32 513		−6.37
TD-B3LYP/6-311++G**	33 337		−4.00
TD-B3PW91/6-311++G**	33 719		−2.90
UHF/6-311++G**		52 768	−19.71
B3LYP/6-311++G**		63 410	−3.52
B3PW91/6-311++G**		63 670	−3.12

2.2. Computational method

Ab initio and DFT calculations were performed to predict molecular structure, energy, vibrational frequency and other properties using the GAUSSIAN 03W [18] program package. Configuration interaction singles (CIS) calculations with the 6-311++G** basis set were applied to predict the vibrational frequencies of indene in the S_1 state. When a scaling factor of 0.91 is applied to approximately correct for the combined errors stemming from basis set incompleteness and negligence of electron correlation and vibrational anharmonicity, the calculated frequencies match well the measured values from the vibronic spectroscopic experiments. The unrestricted Hartree–Fock (UHF) and Becke three-parameter functional with the PW91 correlation functional (UB3PW91) methods were conducted to calculate the vibrational frequencies of the indene cation. When proper scaling factors were applied, the predicted values became very close to the measured frequencies. The IE was obtained as the difference in the zero-point energy (ZPE) levels of the cation and the corresponding neutral.

3. Results

3.1. Vibronic spectrum

Fig. 1 shows the vibronic spectrum of indene in the energy range near its $S_1 \leftarrow S_0$ electronic excitation. To minimize the excess energy produced upon photoionization, the vibronic spectrum was recorded by using the 2C-R2PI technique. It was done by scanning the excitation laser in the range of 34 500–36 200 cm^{-1} while fixing the ionization laser at 31 143 cm^{-1}. The 0^0_0 band appears at 34 725 ± 2 cm^{-1} and general spectral features are nearly identical to those previously reported [12–14]. It is known that the electronic excitation energy may be estimated by the various theoretical calculations. As shown in Table 1, the CIS/6-311++G** procedure predicts this value to be 32 513 cm^{-1}, corresponding

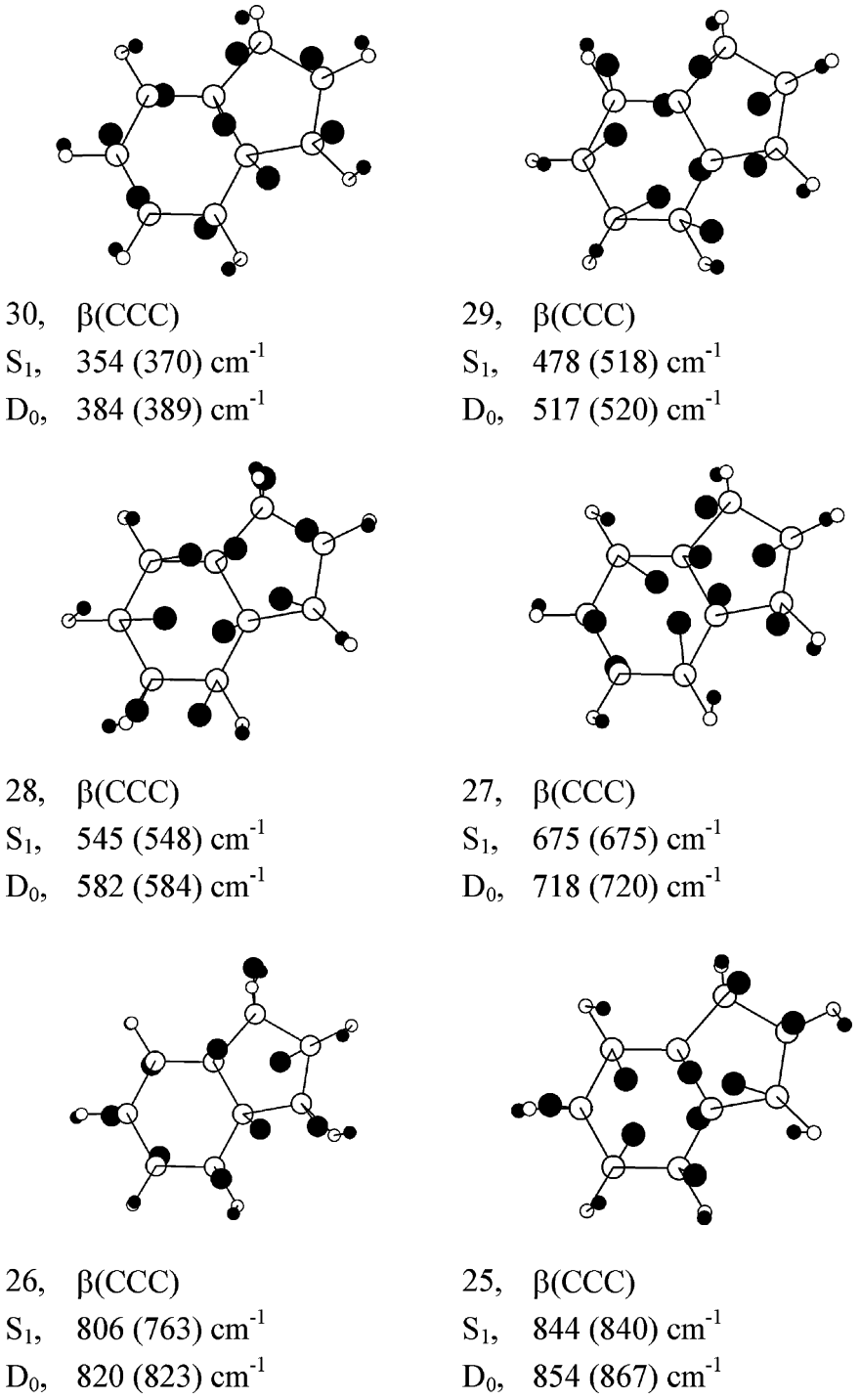

Fig. 2. Some observed active in-plane ring deformation vibrations of indene in the S_1 and D_0 states. The open circles designate the original locations of the atoms, whereas the solid dots mark the displacements. The measured and calculated (in the parentheses) frequencies are included for each mode.

to an underestimation of about 6.37%. In a different approach, the time-dependent hybrid Becke three-parameter Lee–Yang–Parr (TD-B3LYP) functional method with the 6-311++G** basis set gives 33 337 cm^{-1}, corresponding to a difference of 4.00%. When the TD-B3PW91 method is applied, the predicted value becomes 33 719 cm^{-1}, which is lower than the measured value by 2.90%. Therefore, a precise experimental measurement can be used as a goal for theoretical calculations.

The weak band on the low-energy side of the 0_0^0 band in Fig. 1 results from hot band transition. The moderately intense bands at 354, 478, 545, 675, 806, 844, and 945 cm^{-1} are assigned to the 30_0^1, 29_0^1, 28_0^1, 27_0^1, 26_0^1, 25_0^1, and 23_0^1 transitions, respectively, which mainly involve in-plane ring deformation vibrations of indene, as illustrated in Fig. 2. The normal vibrations can be viewed by using the GAUSSVIEW program which is a complementary program for being used with the GAUSSIAN 03W package. Modes 29, 28, and 27 of indene have patterns similar to the in-plane ring deformation vibrations 6a, 6b and 1 of benzene derivatives.

3.2. Cation spectra

We have applied both 2C-R2PI and MATI techniques to record the photoionization efficiency (PIE) curve and vibrationally

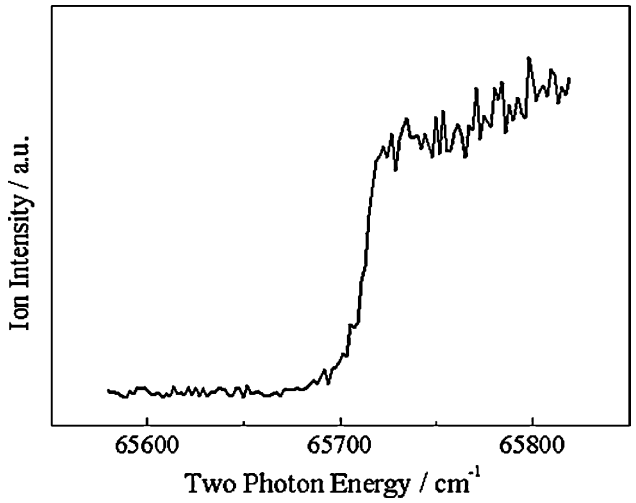

Fig. 3. PIE curve of indene recorded by ionizing via the $S_1 0^0$ intermediate state.

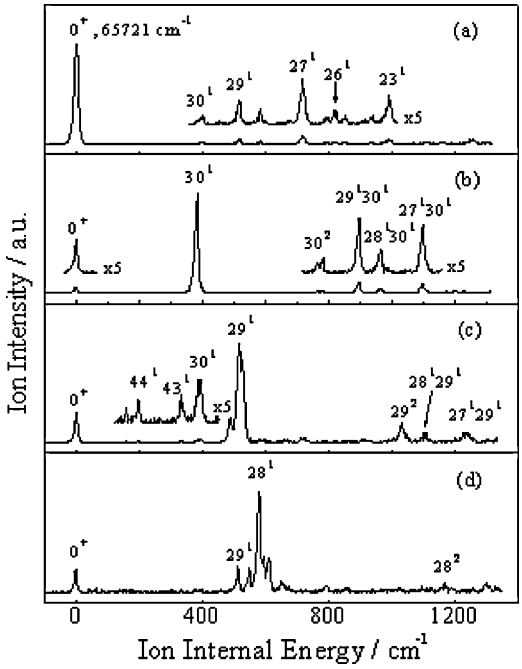

Fig. 4. MATI spectra of indene recorded by ionizing via the (a) 0^0, (b) 30^1, (c) 29^1, and (d) 28^1 intermediate levels in the S_1 state, respectively.

resolved cation spectra of indene. It is noted that this 2C-R2PI procedure is different from that for recording the vibronic spectrum stated in the previous section. The present 2C-R2PI experiment was performed by scanning the ionization laser while fixing the frequency of the excitation laser at the $S_1 0^0$ level. Fig. 3 shows the PIE curve, where the abruptly rising step near 65 715 cm^{-1} indicates the IE of this molecule. Because the 2C-R2PI experiment is subject to detect the non-energy-selected ions, it can hardly give information about the internal motions of the cation. In contrast, the MATI experiment involves detection of the ZEKE ions.

Figs. 4 and 5 depict the MATI spectra of indene recorded by ionizing via the 0^0 (34 725 cm^{-1}), 30^1 ($0^0 + 354\ cm^{-1}$), 29^1 ($0^0 + 478\ cm^{-1}$), 28^1 ($0^0 + 545\ cm^{-1}$), 27^1 ($0^0 + 675\ cm^{-1}$), 26^1 ($0^0 + 806\ cm^{-1}$), 25^1 ($0^0 + 844\ cm^{-1}$), and 23^1 ($0^0 + 945\ cm^{-1}$) levels in the S_1 state. Analysis of these 0^+ bands with consideration of the uncertainty in the laser photon energy, the spectral width, and the Stark effect, yields the adiabatic IE of indene to be 65 721 ± 5 cm^{-1}

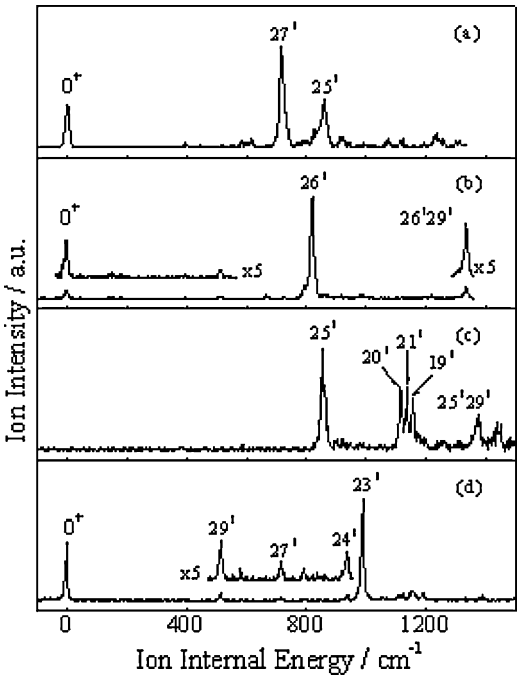

Fig. 5. MATI spectra of indene recorded by ionizing via the (a) 27^1, (b) 26^1, (c) 25^1, and (d) 23^1 intermediate levels in the S_1 state, respectively.

(8.1484 ± 0.0006 eV). Although our measured value is in good agreement with previously reported ones (8.08–8.15 eV [14–16]) on the basis of photoelectron or photoionization experiments, our measurement has a greater precision. As previously mentioned, the MATI technique involves detection of threshold ions with zero kinetic energy. One of the major advantages of this technique over the conventional ion spectroscopic methods is that it can provide information about the internal motions of ions.

The intense MATI bands shifted from the ionization threshold (denoted by 0^+) by 384, 517, 582, 718, 820, 854, and 992 cm^{-1} result from in-plane ring deformation vibrations 30^1, 29^1, 28^1, 27^1, 26^1, 25^1, and 23^1 of the indene cation in the D_0 state, respectively. Although some out-of-plane vibrations are also seen, the intensities of their corresponding MATI bands are relatively weak. The frequencies of the observed bands in Figs. 4 and 5 are listed in Table 2, along with the calculated values and their possible assignments.

4. Discussion

Indene belongs to the symmetry group C_s. By analyzing the UV absorption spectrum, Hollas [12] pointed out that the $S_1 \leftarrow S_0$ electronic excitation is subject to the $\pi^* \leftarrow \pi$ transition. Hartford and Lombardi [13] analyzed rotational structure of the 0_0^0 band. They found that although indene has two out-of-plane hydrogen atoms, its $S_1 \leftarrow S_0$ transition does not have a c-type contribution. It follows that the transition has a hybrid character of 88% *A*-type and 12% *B*-type. Therefore, the transition moment lies in plane and this confirms the $\pi^* \leftarrow \pi$ electronic transition. It follows that the intense vibronic bands must be related to in-plane ring vibrations, as seen in Fig. 1 and that previously reported [14].

As seen in Fig. 4a, when the $S_1 0^0$ state is used as the intermediate level, the only strong MATI feature is the 0^+ band. Most of the weak signals result from the in-plane ring vibrations of the cation. The intensity of the observed MATI band is related to (1) the oscillator strength corresponding to the $S_1 \leftarrow S_0$ transition, (2) the transition cross-section from the S_1 state to the Rydberg state, (3) the pulsed field ionization efficiency, and (4) the overlap integral between the molecular coordinates of the neutral and the cation. To investigate

Table 2
Observed bands (in cm^{-1}) in the MATI spectra of indene and possible assignments.[a]

Intermediate level in the S_1 state								Cal.		Assignment and approximate description [b]
0^0	30^1	29^1	28^1	27^1	26^1	25^1	23^1	UHF	UB3	
158		157						158	155	45^1, ring twisting
195	196	197						201	196	44^1, butterfly
332		333						339	328	43^1, γ(CCC)
401	384	386		398				389	384	30^1, β(CCC)
517		517	513		511		516	520	514	29^1, β(CCC)
583		588	582	582			581	584	581	28^1, β(CCC)
		658	651		667					43^2
717		718		718			719	720	720	27^1, β(CCC)
	765									30^2
822				825	820			823	815	26^1, β(CCC)
854			853	860	864	854		867	850	25^1, β(CCC)
	900									$29^1 30^1$
942				943			936	935	940	24^1, ν(CC)
	966									$28^1 30^1$
993				994	986		992	980	995	23^1, β(vinyl CH)
		1033								29^2
1070				1077			1071	1089	1071	22^1, β(CCC)
	1100									$27^1 30^1$
1114				1122		1113	1121	1125	1114	20^1, β(ring CH)
		1103	1096							$28^1 29^1$
					1134	1135		1160	1159	21^1, β(ring CH)
1159						1153	1158	1178	1155	19^1, β(ring CH)
			1168							28^2
1192	1177			1193			1191	1250	1219	17^1, β(CH_2 CH)
	1205				1200					$26^1 30^1$
	1229									$25^1 30^1$
		1241		1235						$27^1 29^1$
1261	1280						1257	1274	1253	18^1, β(CCC)
1306	1311		1298	1301				1326	1355	16^1, β(CCC)
		1332			1333					$26^1 29^1$
						1373				$25^1 29^1$
						1436				$25^1 28^1$

[a] The experimental values are shifts from 65 721 cm^{-1}, whereas the calculated ones are obtained from the UHF (scaled by 0.94) and the UB3PW91 (scaled by 0.98) calculations using the 6-311+G** basis set.
[b] ν, stretching; β, in-plane ring bending; γ, out-of-plane ring bending.

more active vibrations of the indene cation in the D_0 state and to examine the change of molecular geometry upon ionization, we recorded the MATI spectra by ionization via seven more intermediate vibronic levels. When the vibronic $S_1 30^1$ state is used as the intermediate level, the observed strongest MATI band results from vibrational mode 30 of the indene cation, as seen in Fig. 4b. Similarly, when the $S_1 29^1$, $S_1 28^1$, $S_1 27^1$, $S_1 26^1$, $S_1 25^1$ and $S_1 23^1$ states are used as the intermediate levels, the most intense MATI bands correspond to the same vibrational pattern of the cation, as seen in Figs. 4 and 5. These results indicate that the geometry, symmetry, and vibrational coordinates of the cation in the D_0 state resemble those of the neutral species in the S_1 state for indene. Similar observations have been reported for indole [19] and 1-methylindole [20].

Frequencies of vibrations 30, 29, 28, 27, 26, 25, and 23 are measured to be 384, 517, 582, 718, 820, 854, and 992 cm^{-1} for the indene cation in the D_0 state, respectively. The corresponding frequencies of these seven normal modes are measured to be 354, 478, 545, 675, 806, 844, and 945 cm^{-1} for indene in the neutral electronically excited S_1 state. It is known that frequency is proportional to the square root of force constant. The frequencies of these vibrations of indene in the D_0 state are slightly higher than that in the S_1 state. This indicates that the molecular geometry of indene in the cationic D_0 state is slightly more rigid than that in the neutral S_1 state.

5. Conclusion

We applied 2C-R2PI and MATI techniques to record the vibrational spectra of indene in the S_1 and D_0 states. The band origin of the $S_1 \leftarrow S_0$ electronic transition and the adiabatic IE of indene were found to be $34\,725 \pm 2$ cm^{-1} and $65\,721 \pm 5$ cm^{-1}, respectively. We recorded the MATI spectra by ionization via the 0^0, 30^1, 29^1, 28^1, 27^1, 26^1, 25^1, and 23^1 levels in the S_1 state. Most of the observed active modes in both states are in-plane ring deformation vibrations. Analysis of these MATI spectra suggests that the geometry, symmetry, and vibrational coordinates of the cation in the D_0 state resemble those of the neutral species in the S_1 state. For each of these modes, the frequency in D_0 state is slightly greater than that in the S_1 state. This indicates that indene in the cationic state is slightly more rigid than that in the electronically excited state. Our experimental results show that there is only one isomeric form of this molecule involved in the present photoexcitation and ionization processes. This finding is supported by the ab initio and DFT calculations.

Acknowledgments

We gratefully acknowledge financial support from the National Science Council of the Republic of China under Grant NSC-98-2113-M-001-023-MY3.

References

[1] K. Müller-Dethlefs, K.M. Sander, E.W. Schlag, Chem. Phys. Lett. 112 (1984) 291–294.
[2] K. Müller-Dethlefs, O. Dopfer, T.G. Wright, Chem. Rev. 94 (1994) 1845–1871.
[3] S. Georgiev, R. Karaminkov, S. Chervenkov, V. Delchev, H.J. Neusser, J. Phys. Chem. A 113 (2009) 12328–12336.
[4] O. Kostko, S.K. Kim, S.R. Leone, M. Ahmed, J. Phys. Chem. A 113 (2009) 14206–14211.

[5] C.E.H. Dessent, S.R. Haines, K. Muller-Dethlefs, Chem. Phys. Lett. 315 (1999) 103–108.
[6] J.L. Lin, L.C.L. Huang, W.B. Tzeng, J. Phys. Chem. A 105 (2001) 11455–11461.
[7] J.F. Southern, L. Schafer, K. Brendhau, H.M. Seip, J. Chem. Phys. 55 (1971) 2418–2421.
[8] Y.S. Li, M.R. Jalilian, J.R. Durig, J. Mol. Struct. 51 (1979) 171–174.
[9] S. Zilberg, S. Kendler, Y. Haas, J. Phys. Chem. 100 (1996) 10869–10874.
[10] E.N. Lewis, V.F. Kalasinsky, I.W. Levin, Anal. Chem. 60 (1988) 2658–2661.
[11] T.L. Smithson, R.A. Shaw, H. Wieser, J. Chem. Phys. 81 (1984) 4281–4287.
[12] J.M. Hollas, Spectrochim. Acta 19 (1963) 753–767.
[13] A. Hartford, J.R. Lombardi, J. Mol. Spectrosc. 34 (1970) 257–265.
[14] S. Kendler, S. Zilberg, Y. Haas, Chem. Phys. Lett. 242 (1995) 139–146.
[15] M.J.S. Dewar, E. Haselbach, S.D. Worley, Proc. R. Soc. London A 315 (1970) 431–442.
[16] L. Klasinc, Pure Appl. Chem. 52 (1980) 1509–1524.
[17] W.B. Tzeng, J.L. Lin, J. Phys. Chem. A 103 (1999) 8612–8619.
[18] M.J. Frisch, et al., GAUSSIAN 03, Revision B.01, Gaussian Inc., Pittsburgh, PA, 2003.
[19] T. Vondrak, S. Sato, K. Kimura, J. Phys. Chem. A 101 (1997) 2384–2389.
[20] J.L. Lin, W.B. Tzeng, Chem. Phys. Lett. 377 (2003) 620–626.